ChemComm

Accepted Manuscript

This article can be cited before page numbers have been issued, to do this please use: M. Mori, Y. Fujikawa, M. Kikkawa, M. Shino, M. Sawane, S. Sato and H. Inoue, *Chem. Commun.*, 2019, DOI: 10.1039/C9CC03064F.

ROYAL SOCIETY OF CHEMISTRY

rsc.li/chemcomm

ChemComm

View Article Online
DOI: 10.1039/C9CC03064F

COMMUNICATION

A highly selective fluorogenic substrate for imaging glutathione S-transferase P1: development, and cellular applicability to epigenetic studies†

Received 00th January 20xx,
Accepted 00th January 20xx

DOI: 10.1039/x0xx00000x

Masay Mori, Yuuta Fujikawa,* Manami Kikkawa, Moeho Shino, Mei Sawane, Shiho Sato, and Hideshi Inoue

Pi-class glutathione S-transferase (GSTP1) is a molecular marker enzyme whose expression level is altered in various malignant tumour tissues. Herein, we report the first highly selective fluorogenic GSTP1 substrate, Ps-TG, and its membrane-permeable derivative Ps-TAc, for specific visualization of intracellular GSTP1 activity in cancer cells or epigentically regulated GSTP1 expression.

Enzymes play essential roles as biological catalysts in most physiological and pathological contexts. Therefore, methods for detecting or visualising the activity of a specific enzyme at the single-cell level are valuable[1]. For example, the visualization of cancer-associated enzyme activity using fluorogenic substrates with higher sensitivity and specificity than existing substrates would facilitate the accurate detection of small tumours. Various "smart" (activatable) fluorogenic substrates have been reported to enable the early diagnosis of tumours on a molecular basis and to allow determination of the need for subsequent therapeutic intervention[2–5] and monitoring of the effects of therapeutic intervention. However, it is still difficult to target or visualise the activity of a single specific enzyme from others with similar activity.

Glutathione S-transferases (GSTs) are a group of multifunctional enzymes that catalyse the nucleophilic attack of reduced glutathione (GSH) on electrophiles such as halonitroaromatics and α,β-unsaturated carbonyls, thereby detoxifying endogenously generated or exogenous reactive electrophiles to protect cells from the formation of undesirable protein or nucleotide adducts[6]. The human soluble GSTs are categorized into eight classes (Alpha, Mu, Pi, Theta, Omega, Sigma, Kappa, and Zeta) based on their amino acid sequence similarity. It is known that the Pi-class GST GSTP1 is frequently and highly expressed in a variety of solid tumours[7–12] as well as in benign or pre-neoplastic lesions of colon cancer[13]. Several reports have shown that GSTP1 is a crucial factor for tumorigenesis and tumour growth, based on the fact that *GSTP1* knockout or knockdown has a negative effect on the viability or proliferation rate of cancer cells[9,14]. On the other hand, loss or reduction of GSTP1 expression compared to that of the surrounding normal cells has often been observed in several types of cancers, including prostate cancer. The loss of GSTP1 expression results from the aberrant hypermethylation of CpG islands in the promoter region of the *GSTP1* gene[15,16]. Therefore, the hypermethylation of CpG islands in the *GSTP1* promoter, and the resulting disappearance of GSTP1 expression, can serve as a molecular marker for the detection and diagnosis of prostate and several other cancers[16]. In addition, restored expression of the GSTP1 protein by treatment with epigenetic drugs has been suggested to be a marker of the efficacy of drug treatment in some types of tumours[17,18].

The detection and visualisation of altered GSTP1 activity in cancer cells would therefore be useful for cancer diagnosis and assessment of the efficacy of drug treatment. However, fluorogenic substrates reported to date[19-24] are not suitable for the selective visualisation of GSTP1 activity in living cells due to their lack of GSTP1 selectivity or rapid non-enzymatic background reaction with GSH. Thus, to our knowledge, currently no optimal fluorogenic substrate is available for real-time and selective visualization of intracellular GSTP1 activity.

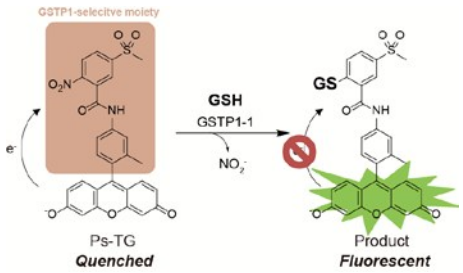

Fig. 1 Fluorescence activation of **Ps-TG** by GSTP1-selective glutathionylation. Before the reaction, the fluorescence of Ps-TG is quenched by photo-induced electron transfer. After replacement of the nitro group with GSH by GSTP1 catalysis, quenching is cancelled, resulting in enhanced fluorescence.

School of Life Sciences, Tokyo University of Pharmacy and Life Sciences, 1432-1 Horinouchi, Hachioji, Tokyo, 192-0392 (Japan) E-mail: yfuji@toyaku.ac.jp
†Electronic Supplementary Information (ESI) available: [details of any supplementary information available should be included here]. See DOI: 10.1039/x0xx00000x

View Article Online

Herein, we report the development and biological application of the first highly selective fluorogenic GSTP1 substrate, **Ps-TG**. Among the previously reported GST substrates, 3,4-dinitrobenzanilide was used as a fluorescence-modulating moiety that enables photo-induced electron transfer (d-PeT) quenching (**Fig. S1**)[22,24,25]. However, both the lack of subtype selectivity and the non-enzymatic background reaction with intracellular GSH (e.g., 0.5-10 mM[26]) hampered selective imaging of GSTP1 activity under physiological conditions. To overcome these drawbacks, we examined a series of nitroaromatics and identified 5-mesyl-2-nitrobenzalinide as a GSTP1-selective substrate (**Fig. 1**). The kinetic and electrochemical properties of 5-mesyl-2-nitrobenzalinide were characterized, as shown in **Figs. S2-S3** and **Table S1** (see Electronic Supplementary Information). Based on these results, **Ps-TG** was designed by coupling the 5-mesyl-2-nitrobenzanilide fluorescence-modulating moiety with the TokyoGreen (TG) fluorophore moiety. The synthetic route for Ps-TG and characterisation of each molecule by ^{1}H-NMR, ^{13}C-NMR, and HRMS are detailed in the Supporting Information. **Ps-TG** showed an absorption and emission maximum at 493 nm and 510 nm, respectively, and a very weak fluorescence signal with a quantum efficiency (QE) of 0.008 due to d-PeT quenching (**Fig. 2A**, **Table S1**). Fluorescence was dramatically enhanced up to a QE of 0.76 (about a 95-fold enhancement) upon GSH conjugation catalysed by GSTP1 (**Table S2**). The glutathionylated product was confirmed by HPLC and LC-MS analyses (**Fig. S4**). The detection limit of GSTP1-1 was determined to be 0.115 ng/ml (**Fig. S5**). Non-enzymatic reaction with GSH was minimal even at high concentrations of GSH up to 20 mM at pH 7.4 (**Fig. S6**). Based on the pH dependence of the spectra, the pK_a values of the phenolic group were 6.2 for Ps-TG and 6.3 for the fluorescent product (**Figs. S7** and **S8**), suggesting that fluorescence intensity is stable around physiological pH. The apparent specificity constant (app. k_{cat}/K_M) for **Ps-TG** was determined to be $(11.0 \pm 0.3) \times$

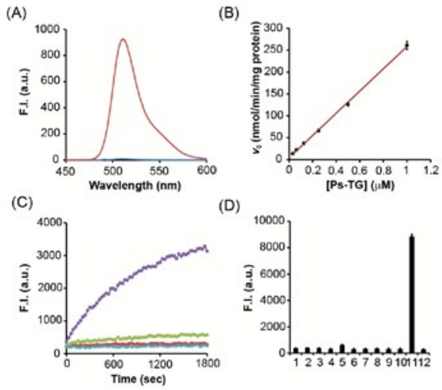

Fig. 2 (A) Fluorescence spectra of 2 μM **Ps-TG** in sodium phosphate buffer (pH 7.4) before (cyan) and after (magenta) reaction. Ex 490 nm. (B) Relationship between the substrate concentration and the specific activity of GSTP1-1 toward **Ps-TG** in the presence of 1 mM GSH in sodium phosphate buffer (100 mM, pH 7.4) at 25°C. (C) Time course of the change in fluorescence intensity of **Ps-TG** (2 μM) by GST catalysis (1 μg/ml) in the presence of 1 mM GSH. Ex 490 nm, Em 510 nm. Data are shown as dots and lines as follows: red, GSTA1-1; green, GSTM1-1; purple, GSTP1-1; cyan, no GST. (D) Reactivity of Ps-TG with various redox active species (1 mM). 1. GSH, 2. DTT, 3. L-cysteine, 4. 2-mercaptoethanol, 5. Na_2S_3, 6. NADH, 7. NAD^+, 8. NADPH, 9. $NADP^+$, 10. ascorbic acid, 11. GSH/GSTP1-1, 12. none.

10^4 $M^{-1}s^{-1}$ based on the linear relationship between the substrate concentration and the initial rate of product formation at 0.13-1.0 μM **Ps-TG** and 1 mM GSH (**Fig. 2B**, **Table S3**). The app. k_{cat}/K_M value for **Ps-TG** is comparable to that determined for the previously characterized GSTP1-1 substrate FOMe-Ac[23] [$(9.5 \pm 0.3) \times 10^4$ $M^{-1}s^{-1}$], but seventy-fold smaller than that determined for the non-selective fluorogenic substrate 3,4-DNADCF[24] [$(690 \pm 100) \times 10^4$ $M^{-1}s^{-1}$]. The app. k_{cat}/K_M value for **Ps-TG** of GSTM1-1 was $(0.94 \pm 0.08) \times 10^4$ $M^{-1}s^{-1}$, which is ten-times smaller than that of GSTP1-1. Thus, **Ps-TG** is a preferred substrate for GSTP1-1 compared to GSTM1-1 (**Fig. 2C**).

Incubation of **Ps-TG** with various reductants showed only negligible increases in fluorescence (**Fig. 2D, Fig. S9**), suggesting essentially no false activation of **Ps-TG** by these molecules. Taken together, these results suggested the effectiveness of **Ps-TG** as a selective and specific fluorogenic substrate for the detection of GSTP1 catalytic activity *in vitro*. Although **Ps-TG** was loaded onto cells expressing GSTP1, no fluorescence activation was observed, presumably due to the lack of membrane permeability by **Ps-TG** (**Fig. S10**). Therefore, the phenol group of **Ps-TG** was acylated to obtain **Ps-TAc** with sufficiently increased hydrophobicity to freely pass through the plasma membrane (**Fig. 3A**). Absorbance spectrum changes confirmed that **Ps-TAc** was deacetylated by incubation with porcine liver esterase (PLE) or with GSH at room temperature (**Fig. S11**), suggesting that **Ps-TAc** is converted to **Ps-TG** after entering the cells. The applicability of **Ps-TAc** as an imaging probe was demonstrated in MCF7 cells transiently transfected with a GSTP1-encoding fusion gene. When the cells transfected with pIRES2-DsRed/3×FLAG-GSTP1 were loaded with 2.5 μM **Ps-TAc**, an intense green fluorescence signal was observed exclusively in the DsRed-positive cells (**Fig. 3B**). This suggests that **Ps-TAc** efficiently enters the cells and becomes a substrate for GSTP1. To further investigate subtype-selectivity in living cells, we tested human GST enzymes, including eighteen subtypes from the eight classes. First, MCF7 cells forcibly

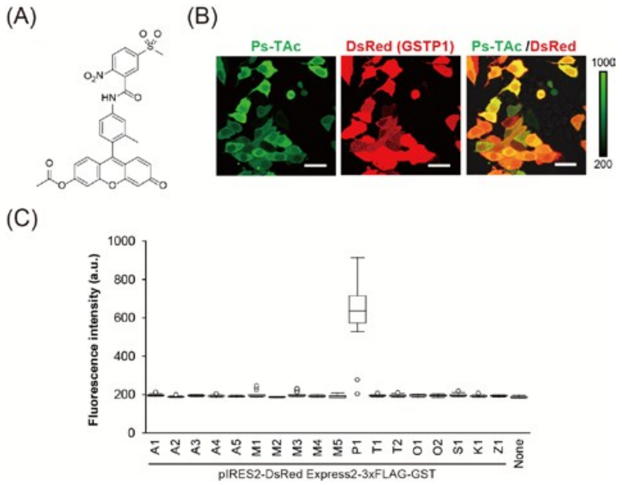

Fig. 3 (A) Molecular structure of **Ps-TAc**. (B) Representative fluorescence images and their merged image of MCF7 cells transfected with pIRES2 DsRed-Express2/3×FLAG-GSTP1 and loaded with 2.5 μM **Ps-TAc** in HBSS at room temperature for 5 min. Scale bars: 40 μm. (B) Box-whisker plot representation of green fluorescence intensity in cells expressing DsRed. n = 60 cells.

View Article Online
DOI: 10.1039/C9CC03064F

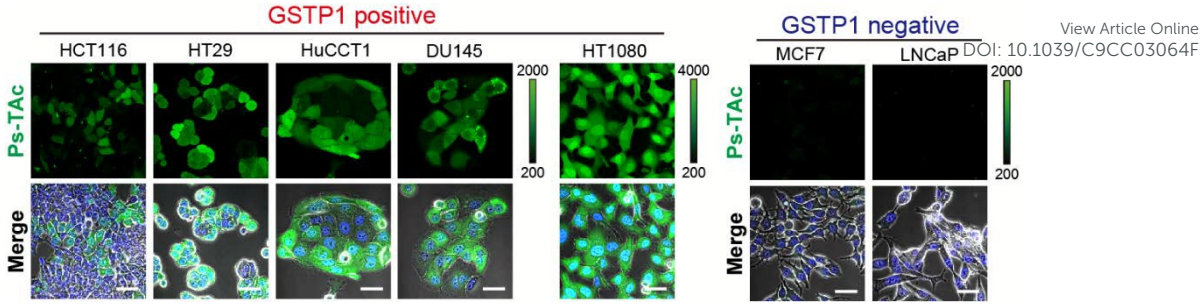

Fig. 4 Various cancer cell lines stained with **Ps-TAc** (upper panels). The **Ps-TAc** fluorescence images (green) were merged with the corresponding images of nuclei (blue) and bright-field images (grey) in various cancer cells (lower panels). Each cell line was incubated with 2.5 μM **Ps-TAc** in HBSS at room temperature for 15 min, and fluorescence and bright-field images were acquired without removing excess fluorogenic substrate. Scale bars: 40 μm.

expressing GST were prepared for each GST subtype (**Fig. S12A**). Expression was exclusively observed in the DsRed-positive cells (**Fig. S12B**). Then, the transfected MCF7 cells were loaded with **Ps-TAc** and subjected to fluorescence imaging using confocal microscopy. DsRed-positive cells were randomly analysed. Notably, an intense green fluorescence signal was observed only in the DsRed-positive cells (**Fig. 3C**). Thus, it was demonstrated that **Ps-TAc** shows unprecedented selectivity as an imaging probe for GSTP1 activity.

Next, to demonstrate its applicability to the visualisation of endogenous GSTP1 activity in tumour cells, **Ps-TAc** was loaded onto various types of cancer cells with or without GSTP1 expression. Remarkable fluorescence was observed in the GSTP1-positive cells HT29, HCT116, HuCCT1, DU145 and HT-1080, but not in the GST-negative cells MCF7 and LNCaP (**Fig. 4**). Note that the staining patterns (e.g., fluorescence intensity, subcellular localization of the fluorescent product) of GSTP1-positive cells were very heterogeneous within a single cell line; there was a large difference in fluorescence intensity among individual cells. Treatment with short interfering RNA (siRNA) against *GSTP1* markedly decreased the fluorescence signal concomitantly with decreased GSTP1 expression in DU145 and HT-1080 cells (**Fig. S13**), consistent with the inference that fluorescence should reflect intracellular GSTP1 activity. Taken together, these results establish that **Ps-TAc** can be used to visualise GSTP1 activity at the single-cell level and to visualise subcellular localization of the glutathionylated product.

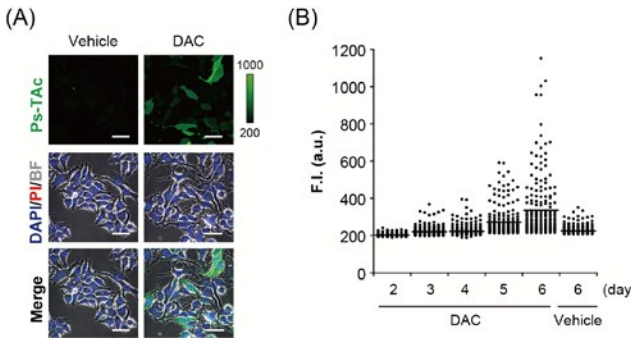

Fig. 5 Visualization of GSTP1 expression in MCF7 cells treated with DAC. (A) Fluorescence (upper panels) and merged (lower panels) with bright-field (BF) images (middle panels) of MCF7 cells treated with 1.25 μM DAC or vehicle for 6 days. Cells were stained with 2.5 μM **Ps-TAc** and 10 μg/ml Hoechst 33258 for 20 min. Images were taken in HBSS containing 10 μg/ml propidium iodide (PI). Scale bars: 40 μm. (B) Dot plot representation of the green fluorescence intensity in MCF7 cells treated with DAC (n = 200 cells/each lane).

The applicability of **Ps-TAc** to the analysis of epigenetic regulation of GSTP1 expression was also examined. Several cancer cell lines have been reported to lack GSTP1 expression due to aberrant hypermethylation of CpG islands in the *GSTP1* promoter region[16]. Treatment with decitabine (DAC), an inhibitor of DNA methylation, is expected to lead to GSTP1 expression in cells where the expression of GSTP1 is repressed due to hypermethylation in the promoter region[27]. Previous reports suggested that restored GSTP1 expression can be used as a marker of the efficacy of epigenetic drugs *in vitro*[17,28] and *in vivo*[18]. In assessing the efficacy of DNA demethylating agents, direct (e.g., bisulphate sequencing, methylation-sensitive restriction fingerprinting, chromatin immunoprecipitation on DNA microarray)[29] and indirect methods (e.g., detection of re-expression of target genes by qPCR, immunoblotting) have been used to evaluate changes in the methylation levels of target genes. None of these methods, however, are applicable to live cells and give information on re-expression of the target gene with single cell resolution. To investigate whether **Ps-TAc** is applicable to assessing the effect of epigenetic drugs based on the GSTP1 re-expression level, MCF7 cells were treated with the epigenetic drug DAC for 2-6 days. At each day of treatment, cells were stained with **Ps-TAc** and subjected to fluorescence confocal microscopic imaging (**Fig. 5**). The fluorescence activation of **Ps-TAc** increased daily in cells treated with 1.25 μM DAC whereas the fluorescence signal was only background level in non-treated cells, even on day 6 (**Fig. 5B**). Propidium iodide (PI) staining showed no significant increase in dead cells following DAC treatment. Increased levels of GSTP1 protein upon DAC treatment were confirmed by immunoblot analysis and immunofluorescence staining (**Fig. S14**). *GSTP1* knockdown with siRNA resulted in a significant decrease in fluorescence activation of **Ps-TAc** in the DAC-treated cells. These results suggest that fluorescence activation of **Ps-TAc** in the DAC-treated cells is due to de-repression of GSTP1 expression by the demethylation of CpG islands (**Fig. S15**). Collectively, these results demonstrated the utility of **Ps-TAc** as an imaging agent to visualise and assess the effect of an epigenetic drug at the single cell level based on the GSTP1 expression level. Sorting cells with strong from very low fluorescence using a fluorescence activated cell sorter (FACS) based on probe fluorescence would allow further analysis of the action of epigenetic drugs at the single cell level or subsequent investigation of tumorigenicity[30]. Therefore, probes with characteristics more suitable for FACS analysis are currently under development and will be reported elsewhere.

In this study, **Ps-TAc**, a plasma membrane-permeable **Ps-TG** derivative, was developed and demonstrated to be applicable to the selective imaging of GSTP1 activity in living cells. The markedly high selectivity of **Ps-TAc** for GSTP1 allows **Ps-TAc** to visualise endogenously expressed GSTP1 at the single cell level. Consequently, **Ps-TAc** holds promise for detecting GSTP1-positive cancer cells and assessing the effect of an epigenetic drug based on its de-repressing activity toward epigenetically silenced GSTP1 expression. Thus, this study presents a new fluorogenic substrate as a powerful chemical tool for investigation of the biological significance of intracellular GSTP1 activity, for the detection of cancer cells, and for assessing epigenetic drugs.

We thank Dr. Toru Komatsu (The University of Tokyo, Japan) for critical discussions; Professor Hisanaka Ito (Tokyo University of Pharmacy and Life Sciences) for support in organic synthesis and spectroscopic measurements; and Dr. Tasuku Ueno (The University of Tokyo, Japan) for cyclic voltammetry measurements and critical discussions. This research was supported by the Platform Project for Supporting Drug Discovery and Life Science Research (Platform for Drug Discovery, Informatics, and Structural Life Science) from the Japan Agency for Medical Research and Development (AMED); by the Private University Research Branding Project of the Japanese Ministry of Education, Culture, Sports, Science and Technology; by MEXT/JSPS KAKENHI (18K05362); and by the Science Research Promotion Fund from The Promotion and Mutual Aid Corporation for Private Schools of Japan (to Y.F.).

Conflicts of interest

There are no conflicts to declare.

References

1 H. Kobayashi, M. Ogawa, R. Alford, P. L. Choyke, Y. Urano, *Chem. Rev*. 2010, **110**, 2620.
2 N. Muguruma, K. Okamoto, T. Nakagawa, K. Sannomiya, S. Fujimoto, Y. Mitsui, T. Kimura, H. Miyamoto, J. Higashijima, M. Shimada, Y. Horino, S. Matsumoto, K. Hanaoka, T. Nagano, M. Shibutani, T. Takayama, *Sci. Rep*. 2017, **7**, 6536.
3 H. Onoyama, M. Kamiya, Y. Kuriki, T. Komatsu, H. Abe, Y. Tsuji, K. Yagi, Y. Yamagata, S. Aikou, M. Nishida, K. Mori, H. Yamashita, M. Fujishiro, S. Nomura, N. Shimizu, M. Fukuyama, K. Koike, Y. Urano, Y. Seto, *Sci. Rep*. 2016, **6**, 1.
4 H. J. Knox, J. Hedhli, T. W. Kim, K. Khalili, L. W. Dobrucki, J. Chan. *Nat Commun*. 2017, **8**, 1794.
5 X. Wang, P. Li, Q. Ding, C. Wu, W. Zhang, B. Tang. *J Am Chem Soc*. 2019, **141**, 2061.
6 J. D. Hayes, J. U. Flanagan, I. R. Jowsey, *Annu. Rev. Pharmacol. Toxicol.* 2005, **45,** 51.
7 J. A. Moscow, C. R. Fairchild, M. J. Madden, D. T. Ransom, H. S. Wieand, E. E. O'Brien, D. G. Poplack, J. Cossman, C. E. Myers, K. H. Cowan, *Cancer Res.* 1989, **49**, 1422.
8 C. D. Illio, G. D. Boccio, A. Aceto, R. Casaccia, F. Mucilli, G. Federici, *Carcinogenesis* 1988, **9**, 335.
9 D. T. Dang, F. Chen, M. Kohli, C. Rago, J. M. Cummins, L. H. Dang, *Cancer Res.* 2005, **65**, 9485.
10 C.Kodate, A. Fukushi, T. Narita, H. Kudo, Y. Soma, K. Sato, *Jpn. J. Cancer Res.* 1986, **77**, 226-229.
11 M. K. Kelley, A. Engqvist-Goldstein, J. A. Montali, J. B. Wheatley, D. E. Schmidt, L. M. Kauvar, *Biochem. J.* 1994, **304**, 843.
12 Y. Shiratori, Y. Soma, H. Maruyama, S. Sato, A. Takano, K. Sato, *Cancer Res.* 1987, **47**, 6806.
13 K. Miyanishi, T. Takayama, M. Ohi, T. Hayashi, A. Nobuoka, T. Nakajima, R. Takimoto, K. Kogawa, J. Kato, S. Sakamaki, Y. Niitsu, *Gastroenterology* 2001, **121**, 865.
14 M. Mutallip, N. Nohata, T. Hanazawa, N. Kikkawa, S. Horiguchi, L. Fujimura, K. Kawakami, T. Chiyomaru, H. Enokida, M. Nakagawa, Okamoto, Y. Seki, N. *Int. J. Mol. Med*. 2011, **27**, 345.
15 D. S. Millar, K. Ow, C. L. Paul, P. J. Russell, P. L. Molloy, S. J. Clark, *Oncogene* 1999, **18**, 1313.
16 M. Schnekenburger, T. Karius, M. Diederich, *Front. Pharmacol*. 2014, **5**, 1.
17 K. Chiam, M. M. Centenera, L. M. Butler, W. D. Tilley, T. Bianco-Miotto, *PLoS One* 2011, **6**, e25634.
18 X. Yu, B. S. Cornblatt, A. Kumar, S. Piantadosi, T. L. DeWeese, A. M. De Marzo, W. G. Nelson, *Cancer Res*. 2001, **61**, 8611.
19 J. Zhang, A. Shibata, M. Ito, S. Shuto, Y. Ito, B. Mannervik, H. Abe, R. Morgenstern, *J. Am. Chem. Soc.* 2011, **133**, 14109.
20 A. Shibata, Y. Nakano, M. Ito, M. Araki, J. Zhang, Y. Yoshida, S. Shuto, B. Mannervik, R Mogenstern, Y. Ito, H. Abe, *Analyst* 2013, **138**, 7326.
21 J. Zhang, Z. Jin, X. X. Hu, H. M. Meng, J. Li, X. B. Zhang, H. W. Liu, T. Deng, S. Yao, L. Feng, *Anal. Chem.* 2017, **89**, 8097.
22 Y. Fujikawa, Y. Urano, T. Komatsu, K. Hanaoka, H. Kojima, T. Terai, H. Inoue, T. Nagano, *J. Am. Chem. Soc.* 2008, **130**, 14533.
23 Y. Fujikawa, T. Nampo, M. Mori, M. Kikkawa, H. Inoue, *Talanta* 2018, **179**, 845.
24 Y. Fujikawa, F. Morisaki, A. Ogura, K. Morohashi, S. Enya, R. Niwa, S. Goto, H. Kojima, T. Okabe, T. Nagano, H. Inoue, *Chem. Commun.* 2015, **51**, 11459.
25 T. Ueno, Y. Urano, K. Setsukinai, H. Takakusa, H. Kojima, K. Kikuchi, K. Ohkubo, S. Fukuzumi, T. Nagano, *J. Am. Chem. Soc.* 2004, **126**, 10640.
26 A. Meister, M. E. Anderson, *Annu. Rev. Biochem.* 1983, **52**, 711.
27 M. Szyf, *Biochim. Biophys. Acta* 2010, **1799**, 750.
28 M. Pandey, S. Shukla, S. Gupta, *Int. J. Cancer* 2010, **126**, 2520.
29 S.Majumdar, Buckles E, Estrada J, Koochekpour S. *Curr. Genomics* 2011, **12**, 486.
30 H. C. Tsai, H. Li, L. Van Neste, Y. Cai, C. Robert, F. V. Rassool, J. J. Shin, K. M. Harbom, R. Beaty, E. Pappou, J. Harris, R. W. Yen, N. Ahuja, M. V. Brock, V. Stearns, D. Feller-Kopman, L. B. Yarmus, Y. C. Lin, A. L. Welm, J. P. Issa, I. Minn, W. Matsui, Y. Y. Jang, S. J. Sharkis, S. B. Baylin, C. A. Zahnow, *Cancer Cell* 2012, **21**, 430.

TOC

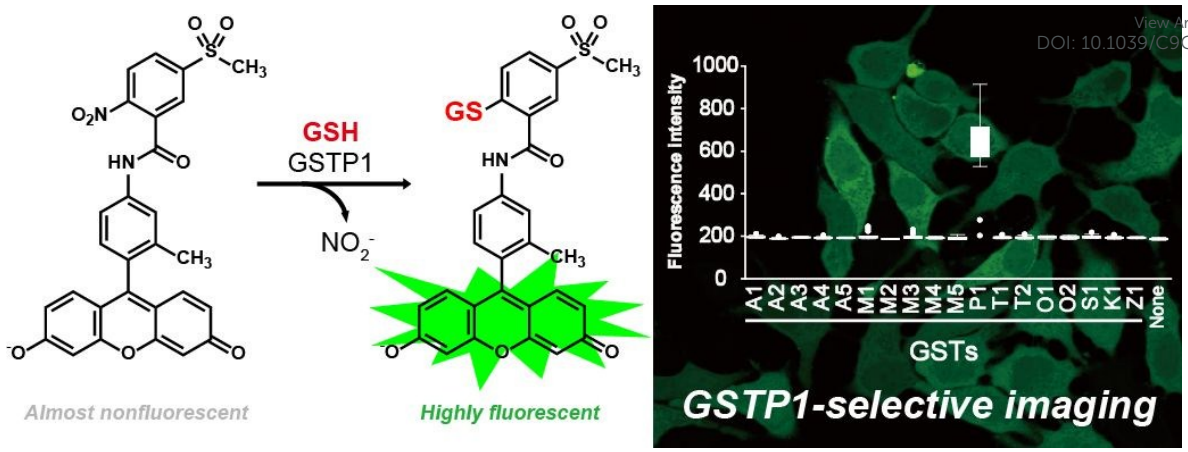

Highly selective fluorogenic substrate was desined for the specific visualization of intracellular GSTP1 activity in cancer cells.